Novel Macrocyclic Eu^{II} Complexes: Fast Water Exchange Related to an Extreme $M-O_{water}$ Distance**

László Burai, Éva Tóth,* Gilles Moreau, Angélique Sour, Rosario Scopelliti, and André E. Merbach[a]

Abstract: Eu^{II} complexes are potential candidates for pO_2-responsive contrast agents in magnetic resonance imaging. In this regard, we have characterized two novel macrocyclic Eu^{II} chelates, $[Eu^{II}(DOTA)(H_2O)]^{2-}$ and $[Eu^{II}(TETA)]^{2-}$ (H_4DOTA = 1,4,7,10-tetraazacyclododecane-1,4,7,10-tetraacetic acid, H_4TETA = 1,4,8,11-tetraazacyclotetradecane-1,4,8,11-tetraacetic acid) in terms of redox and thermodynamic complex stability, proton relaxivity, water exchange, rotation and electron spin relaxation. Additionally, solid-state structures were determined for the Sr^{II} analogues. They revealed no inner-sphere water in the TETA and one inner-sphere water molecule in the DOTA complex. This hydration pattern is retained in solution, as the ^{17}O chemical shifts and ^1H relaxation rates proved for the corresponding Eu^{II} compounds. The thermodynamic complex stability, determined from the formal redox potential and by pH potentiometry, of $[Eu^{II}(DOTA)(H_2O)]^{2-}$ ($\lg K^{Eu(II)} = 16.75$) is the highest among all known Eu^{II} complexes, whereas the redox stabilities of both $[Eu^{II}(DOTA)(H_2O)]^{2-}$ and $[Eu^{II}(TETA)]^{2-}$ are inferior to that of 18-membered macrocyclic Eu^{II} chelates. Variable-temperature ^{17}O NMR, NMRD and EPR studies yielded the rates of water exchange, rotation and electron spin relaxation. Water exchange on $[Eu^{II}(DOTA)(H_2O)]^{2-}$ is remarkably fast ($k_{ex}^{298} = 2.5 \times 10^9\ s^{-1}$). The near zero activation volume ($\Delta V^{\neq} = +0.1 \pm 1.0\ cm^3 mol^{-1}$), determined by variable-pressure ^{17}O NMR spectroscopy, points to an interchange mechanism. The fast water exchange can be related to the low charge density on Eu^{II}, to an unexpectedly long $M-O_{water}$ distance (2.85 Å) and to the consequent interchange mechanism. Electron spin relaxation is considerably slower on $[Eu^{II}(DOTA)(H_2O)]^{2-}$ than on the linear $[Eu^{II}(DTPA)(H_2O)]^{3-}$ (H_5DTPA = diethylenetriaminepentaacetic acid), and this difference is responsible for its 25% higher proton relaxivity (r_1 = 4.32 $mM^{-1}s^{-1}$ for $[Eu^{II}(DOTA)(H_2O)]^{2-}$ versus 3.49 $mM^{-1}s^{-1}$ for $[Eu^{II}(DTPA)(H_2O)]^{3-}$; 20 MHz, 298 K).

Keywords: europium · macrocyclic ligands · MRI contrast agents · NMR spectroscopy · N,O ligands

Introduction

Current research developments in MRI contrast agents aim to visualize the physicochemical state and activity of tissues.[2–3] Such responsive or "smart" contrast agents can report on physiological parameters such as oxygen partial pressure, pH, temperature, intra- and extracellular distributions of ions, metabolite concentration and enzymatic activity. Information on oxygen partial pressure pO_2 in blood or tissue could give insight into metabolic processes of cells, permit the differentiation of arterial and venous blood or show pathological mutation (strokes, tumors, ischemic diseases). The simplest pO_2-responsive contrast agent would be a complex with a redox-active metal center in which one oxidation state is "MRI active" (characterized by strong enhancement of proton relaxation) and the other is "MRI inactive" (weak enhancement of proton relaxation). Thus, MR image intensity will depend on the oxidation state of the metal ion, which is related to the oxygen partial pressure. So far Mn^{III}/Mn^{II} TPPS complexes were reported to have pO_2-dependent proton relaxivities (TPPS = 5,10,15,20-tetrakis(*p*-sulfonatophenyl)-porphinate).[4] The Eu^{II}/Eu^{III} redox system is another candidate for application as a pO_2-responsive contrast agent. Like Gd^{III}, Eu^{II} has seven unpaired electrons, and hence strong relaxation enhancement, while the Eu^{III} ion has a negligible effect on proton relaxation.[5–6] The difficulty with this system, however, resides in the redox instability of the Eu^{II} oxidation state. In the last few years we have characterized several Eu^{II} complexes in terms of redox and thermodynamic complex stability. Parameters that are important for potential use as a

[a] Dr. É. Tóth, Dr. L. Burai, Dr. G. Moreau, Dr. A. Sour, Dr. R. Scopelliti, Prof. A. E. Merbach
Institut de Chimie Moléculaire et Biologique
Ecole Polytechnique Fédérale de Lausanne, EPFL-BCH
1015 Lausanne (Switzerland)
Fax: (+41) 21-693-9875
E-mail: eva.jakabtoth@epfl.ch

[**] High-Pressure NMR Kinetics, Part 100. For Part 99: see ref. [1].

Supporting information for this article is available on the WWW under http://www.wiley-vch.de/home/chemeurj.org/ or from the author.

0947-6539/03/0906-1394 $ 20.00+.50/0

pO_2-responsive contrast agent, such as the rates of water exchange and electronic relaxation, were also determined.[7–10] In addition, we obtained the first solid-state X-ray structure for a Eu^{II} poly(amino carboxylate) chelate, namely, $[Eu^{II}(DTPA)(H_2O)]^{3-}$. In comparison to the Gd^{III} complexes, the Eu^{II} analogues have faster water exchange, and usually faster electronic relaxation. Eighteen-membered macrocyclic chelators such as $ODDA^{2-}$ and $ODDM^{4-}$ (Scheme 1) were found to better protect Eu^{II} from oxidation than linear ligands. The Eu^{II} cryptate complex formed with the cryptand

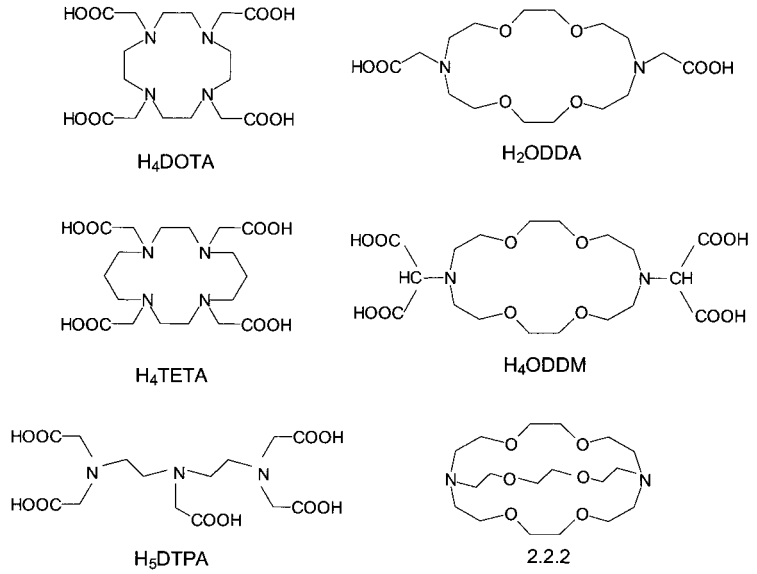

Scheme 1. Macrocyclic ligands used in this study.

4,7,13,16,21,24-hexaoxa-1,10-diazabicyclo[8.8.8]hexacosane (2.2.2) has the highest redox stability among all chelates studied. In a preliminary communication, it was shown that $[Eu^{II}(2.2.2)(H_2O)_2]^{2+}$ has several interesting features with respect to pO_2-responsive MRI contrast agents. In addition to its relative stability against oxidation, it has two inner-sphere water molecules, and water exchange and electron spin relaxation rates are in the optimal range to attain high proton relaxivities, provided rotation is also optimized.[10] We have extended these investigations to macrocyclic ligands of varying size: Eu^{II} chelates with the 14-membered $TETA^{4-}$ and the 12-membered $DOTA^{4-}$ were studied. The latter ligand is known as one of the best chelators for a variety of metal ions, including Gd^{III}.

The Eu^{II} ion has an ionic size and charge similar to Sr^{II} (125 and 126 pm, respectively, for coordination number 8),[11] and consequently they show similar coordination chemistry. For instance, practically identical crystal structures (very similar bond lengths and angles) were found for the Sr^{II} and Eu^{II} DTPA complexes, with eight coordinating donor atoms from the ligand and one inner-sphere water molecule.[9] Hence, the structure of a Eu^{II} complex is often deduced from that of the Sr^{II} analogue. Concerning DOTA and TETA complexes, Varnek et al. performed a molecular dynamics study which showed different coordination patterns and hydration numbers for $[Sr(DOTA)]^{2-}$ and $[Sr(TETA)]^{2-}$.[12] $[Sr(TETA)]^{2-}$ was found to be nine-coordinate with one water molecule in the inner coordination sphere, whereas an eight-coordinate structure without inner-sphere water was obtained for $[Sr(DOTA)]^{2-}$.

The objective of the present work was threefold: i) to assess the redox stability and thermodynamic complex stability of $[Eu^{II}(DOTA)]^{2-}$ and $[Eu^{II}(TETA)]^{2-}$ in aqueous solution by cyclovoltammetry and potentiometry, ii) to characterize the two complexes with respect to application as MRI contrast agents, and iii) to obtain information on their solid-state structures. To accomplish these goals, ^1H and ^{17}O relaxation rates were measured on solutions of the Eu^{II} complexes at several magnetic fields and temperatures. This study was coupled with variable-temperature EPR measurements. The crystal structures of $[Sr(DOTA)]^{2-}$ and $[Sr(TETA)]^{2-}$ were also determined. The results are discussed in comparison to previously reported Eu^{II} complexes.

Results and Discussion

Crystal structures of $[C(NH_2)_3]_2[Sr(DOTA)(H_2O)]\cdot 4H_2O$ and $[C(NH_2)_3]_2[Sr(TETA)(H_2O)]\cdot 5H_2O$: In the absence of suitable crystals of $[Eu^{II}(DOTA)]^{2-}$ and $[Eu^{II}(TETA)]^{2-}$, we determined the structure of the corresponding Sr^{II} complexes. The crystallization of Eu^{II} complexes from aqueous solution for X-ray analysis is often problematic due to ready oxidation. It was proved in several cases that crystals of Sr^{II} and Eu^{II} complexes are isomorphic, as a consequence of the close ionic radius and identical charge of the two metal ions.[9, 13] Moreover, recent XAFS studies proved that in aqueous solution Sr^{II} and Eu^{II} chelates adopt identical structures.[14] Therefore Sr^{II} is generally accepted as a surrogate of Eu^{II} in structural studies when suitable crystals of Eu^{II} compounds cannot be obtained.

In $[Sr(DOTA)(H_2O)]^{2-}$ (Figure 1, top), the coordination number of the metal atom is nine, and the coordination geometry of the ligand is a distorted capped twisted square antiprism (TSA, also called minor isomer *m*) with C_4 symmetry. As required by the symmetry, all metal–oxygen and metal–nitrogen bond lengths are identical (Sr–O 2.548(4) Å; Sr–N 2.731(6) Å). The two planes formed by the ring nitrogen atoms and by the carboxylate oxygen atoms below and above the central metal ion are parallel, with an N-Sr1-O twist angle of 23.9° between the N_4 and O_4 planes. The distances of these planes from the Sr^{II} center are 1.735 and 0.815 Å, respectively. The inner-sphere water molecule occupies the ninth coordination site, 2.85(2) Å from the Sr^{II} ion. This $Sr–O_{water}$ distance is remarkably long, 0.23 Å longer

  0947-6539/03/0906-1395 $ 20.00+.50/0

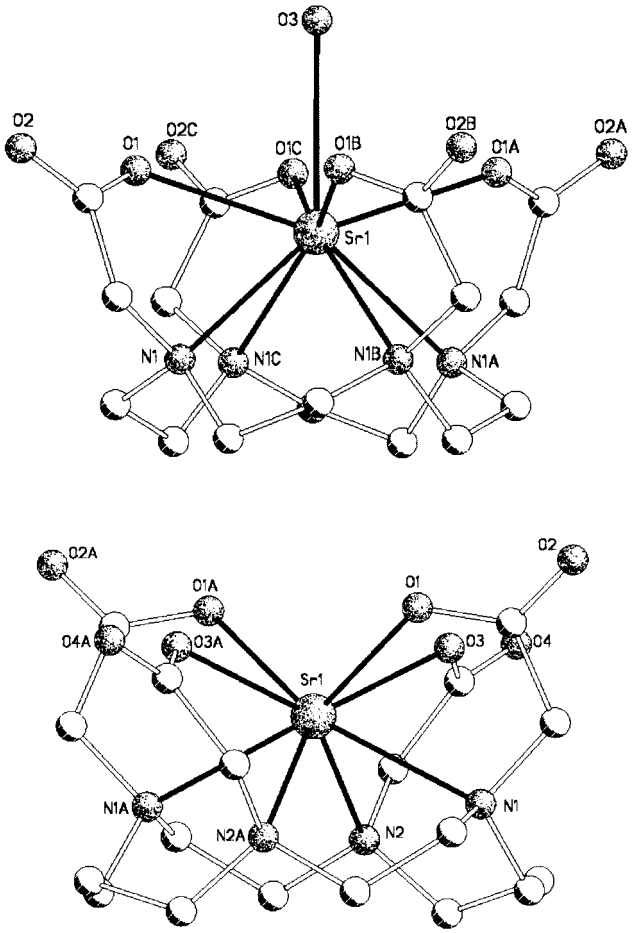

Figure 1. Crystal structures of $[Sr(DOTA)(H_2O)]^{2-}$ (top) and $[Sr(TETA)]^{2-}$ (bottom).

than that in $[Sr(DTPA)(H_2O)]^{3-}$ (and in $[Eu^{II}(DTPA)(H_2O)]^{3-}$).[9] Other Sr^{II} or Eu^{II} chelates also have considerably shorter $M-O_{water}$ distances. For instance, a recent XAFS study in solution found 2.58 Å for $Eu^{II}(aq)$, 2.54 Å for $[Eu^{II}(ODDA)(H_2O)]$, and 2.62 Å for $[Eu^{II}(DTPA)(H_2O)]^{3-}$.[14] This unusually long distance may explain why a previous MD simulation in aqueous solution gave no inner-sphere water molecule in $[Sr(DOTA)]^{2-}$.[12]

On the other hand, the MD simulations showed one water molecule in $[Sr(TETA)]^{2-}$. As the structure in Figure 1 (bottom) shows, $[Sr(TETA)]^{2-}$ has no inner-sphere water in the solid state. The coordination number is eight, and the coordination geometry is a distorted square antiprism with C_2 symmetry. The twofold symmetry axis means that two types of donor oxygen and nitrogen atoms are present (Sr–O1 2.526(2), Sr–O3 2.543(2) Å; Sr–N1 2.742(3), Sr–N2 2.747(3) Å). The average planes of the coordinating oxygen and nitrogen atoms are parallel. Due to the inequivalence of the four Sr–O and four Sr–N distances, there are two different twist angles (22.0° and 31.8°). The distance between Sr^{II} and the N_4 and O_4 mean planes are 1.416 and 1.173 Å, respectively. The O1-Sr1-O1A and O3-Sr1-O3A bond angles are 111.2(1)° and 137.7(1)°, respectively, in $[Sr(TETA)]^{2-}$, while the same angle in $[Sr(DOTA)(H_2O)]^{2-}$ is 142.7(3)°. In contrast to $[Sr(TETA)]^{2-}$, the larger bond angles and the shorter distance of Sr^{II} from the coordinated O_4 plane in $[Sr(DOTA)(H_2O)]^{2-}$ open the ninth coordination site for a water molecule (Figure 2). Gd^{III} and Eu^{III} analogues show similar pattern: in $[Gd(DOTA)(H_2O)]^-$, the $O_{carboxylate}$-Gd-$O_{carboxylate}$ angles are 146°,[15] leaving room for one inner-sphere water molecule, whereas in $[Eu(TETA)]^-$, which has no inner-sphere water, these angles are considerably smaller (104, 131°).[16] Accordingly, the 13-membered macrocyclic chelate $[Gd(TRITA)(H_2O)]^-$ (TRITA = 1,4,7,10-tetraazacyclotridecane-1,4,7,10-tetraacetic acid) has intermediate O-Gd-O bond angles (136.7 and 142.7°) that indicate increased steric crowding around the water-binding site relative to $[Gd(DOTA)(H_2O)]^-$.[17] Some selected bond lengths of the complexes are presented in Table 1 with data for the corresponding Gd^{III} and/or Eu^{III} complexes for comparison.[15, 18–19] As previously observed for $DTPA^{5-}$, the geometry of the Sr^{II} (Eu^{II}) and Gd^{III} complexes is similar for both $DOTA^{4-}$ and $TETA^{4-}$ complexes; only the bond lengths are 0.1-0.2 Å longer in the M^{II} complexes. (Detailed tables of bond lengths and angles in $[Sr(DOTA)(H_2O)]^{2-}$ and $[Sr(TETA)]^{2-}$ are available as Supporting Information.)

Redox and thermodynamic stability of the Eu^{II} complexes: The formal potential $E_{1/2}$ of a $Eu^{III}L/Eu^{II}L$ redox couple gives direct information on the redox stability of the Eu^{II} state: a less negative $E_{1/2}$ indicates higher resistance of $Eu^{II}L$ to oxidation. The formal potential is related to the ratio of the thermodynamic stabilities of $Eu^{III}L$ and $Eu^{II}L$ [Eq. (1)],[20] where $K_{Eu^{III}}$ and $K_{Eu^{II}}$ are the thermodynamic stability constants of the oxidized and reduced forms, respectively. A positive $\Delta E_{1/2}$ value means higher thermodynamic stability of the $Eu^{II}L$ complex relative to its $Eu^{III}L$ analogue.

$$\Delta E_{1/2} = E_{1/2,\text{complexed}} - E_{1/2,\text{uncomplexed}} = \frac{RT}{F}\ln\frac{K_{Eu^{II}}}{K_{Eu^{III}}} \quad (1)$$

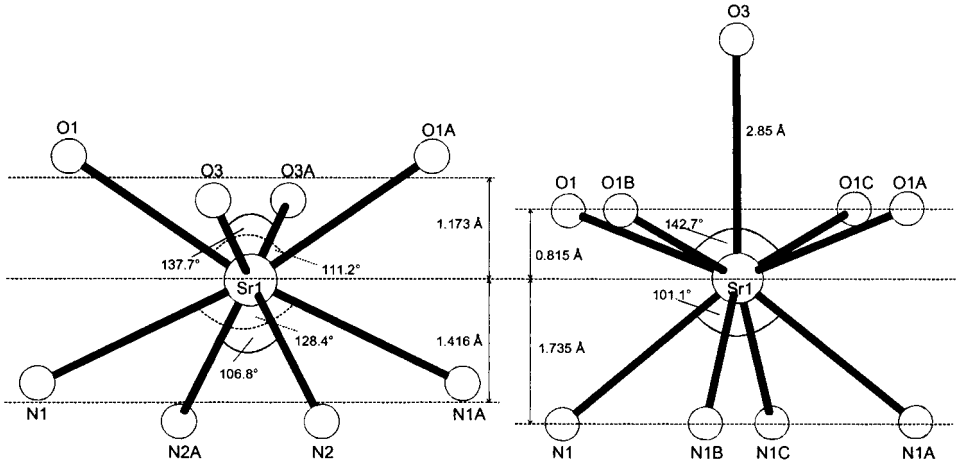

Figure 2. Schematic representation of the coordination polyhedra for $[Sr(DOTA)(H_2O)]^{2-}$ (right) and $[Sr(TETA)]^{2-}$ (left).

Table 1. Solid-state metal to coordinating atom bond lengths determined by X-ray analysis in selected macrocyclic complexes.

Complex	$M-O_{carboxylate}$	M–N	$M-O_{water}$	Ref.
$[Sr(DOTA)(H_2O)]^{2-}$	2.548(4)	2.731(6)	2.849(16)	this work
$[Gd(DOTA)(H_2O)]^{-}$	2.362–2.370	2.648–2.679	2.458	[15a]
$[Eu^{III}(DOTA)(H_2O)]^{-}$	2.247–2.511	2.519–2.900	2.480	[18a]
$[Sr(TETA)]^{2-}$	2.526(2)/2.543(2)	2.742(3)/2.747(3)	–	this work
$[Eu^{III}(TETA)]^{-}$	2.339–2.362	2.579–2.683	–	[19]

The cyclovoltammetric curves of $[Eu^{II}(DOTA)(H_2O)]^{2-}$, $[Eu^{II}(TETA)]^{2}$, and $Eu^{II}(aq)$ are shown in Figure 3. The formal potentials (−1135, −995, and −585 mV versus Ag/AgCl for $[Eu^{II}(DOTA)(H_2O)]^{2-}$, $[Eu^{II}(TETA)]^{2-}$, and Eu^{II}-(aq), respectively) reveal lower stability against oxidation for

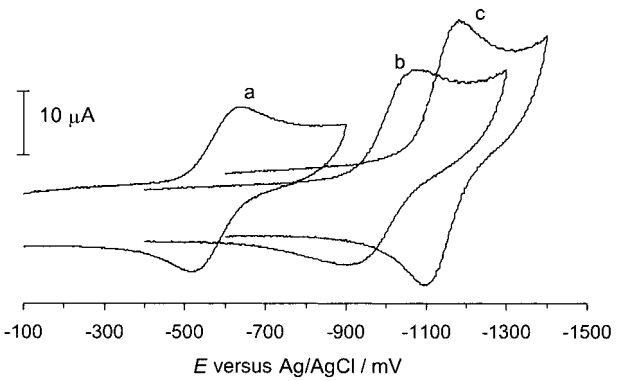

Figure 3. Cyclovoltammograms of $EuCl_3$ (a), $[Eu^{III}(TETA)]^{-}$ (b), and $[Eu^{III}(DOTA)(H_2O)]^{-}$ (c).

these complexes than for the aquated ion. In practice, in an aqueous solution of $[Eu^{II}(DOTA)(H_2O)]^{2-}$ or $[Eu^{II}(TETA)]^{2}$ under nitrogen at room temperature, oxidation is noticeable a few hours after preparation. Table 2 summarizes formal potentials of different Eu^{II} complexes. The potentials of $[Eu^{II}(DOTA)(H_2O)]^{2-}$and $[Eu^{II}(TETA)]^{2-}$ are between the values measured for the complexes of 18-membered diazatetraoxa macrocycles $[Eu^{II}(ODDA)(H_2O)]$ and $[Eu^{II}$-$(ODDM)]^{2-}$ and for the noncyclic $[Eu^{II}(DTPA)(H_2O)]^{3-}$. This may be the consequence of the relatively small 12- and 14-membered rings, in which the smaller Eu^{III} fits better. The four carboxylate groups are also unfavorable for the reduced Eu^{II} state. Presumably, the redox stability of the complexes with 12- and 14-membered tetraaza macrocyclic rings could be also increased by substituting the carboxylates by nitrogen-donor groups. The most redox stable complex found so far is $[Eu^{II}(2.2.2)(H_2O)_2]^{2+}$ ($E_{1/2} = -205$ mV versus SCE).[21] Hence, the stability constant of $[Eu^{II}(2.2.2)(H_2O)_2]^{2+}$ calculated from Equation (1) is approximately 10^7-fold higher than that of the corresponding Eu^{III} complex. Note, however, that it is not sufficient to have a high relative stability of an Eu^{II} complex over its Eu^{III} analogue (expressed by a positive formal potential [Eq. (1)]); the absolute values of both Eu^{II} and Eu^{III} thermodynamic complex stability constants should also be high enough to avoid dissociation and hydrolysis of the Eu^{III} complex following oxidation. Any dissociation of the Eu^{III} or Eu^{II} chelate would further accelerate the oxidation process by displacing the redox equilibrium towards the Eu^{III} state. This phenomenon could result in toxicity problems in in vivo medical application of the Eu^{II} complex as a responsive contrast agent.

The thermodynamic stability constants $\lg K_{Eu^{II}}$ of $[Eu^{II}$-$(DOTA)(H_2O)]^{2-}$ and $[Eu^{II}(TETA)]^{2-}$ were determined by pH potentiometric titration and electrochemically by applying Equation (1). In the analysis of the pH-potentiometric data, previously published values of the ligand protonation constants $\lg K^{H}$ were used (11.22, 9.64, 4.86, 3.68 for $DOTA^{4-}$ and 10.92, 10.09, 4.08, 3.19 for $TETA^{4-}$; $I = 0.1$ M $(CH_3)_4NCl$).[22] For the first $\lg K^{H}$ of $DOTA^{4-}$, a higher value ($\lg K_1^{H} = 12.6$) was recently reported.[23] However, for the sake of comparison between the stability constant determined in this study for $[Eu^{II}(DOTA)(H_2O)]^{2-}$ and that previously published for $[Sr(DOTA)(H_2O)]^{2-}$, we used $\lg K_1^{H} = 11.22$). The use of Equation (1) requires stability constants for the corresponding Eu^{III} complexes. We used $\lg K_{Eu^{III}} = 26.21$ for $[Eu^{III}(DOTA)(H_2O)]^{-}$ and $\lg K_{Eu^{III}} = 14.02$ for $[Eu^{III}$-$(TETA)]^{-}$.[24] For both complexes, the stability constants calculated from the potentiometric data and those from the formal electrode potentials agree well. For $[Eu^{II}$-$(DOTA)(H_2O)]^{2-}$, a complex protonation constant of $\lg K_{ML}^{H} = 4.17 \pm 0.13$ was measured, which is comparable to the literature value of 4.52 for $[Sr(DOTA)(H_2O)]^{2-}$.[22]

Table 2 also presents the $\lg K$ values for the corresponding Sr^{II} ($\lg K^{Sr}$) and Gd^{III} ($\lg K^{Gd}$) complexes.[25–27] As usual, $\lg K$ of the Eu^{II} complexes are slightly higher than those of the Sr^{II} analogues. The thermodynamic stability of $[Eu^{II}$-$(DOTA)(H_2O)]^{2-}$ is the highest among all Eu^{II} complexes studied so far. Nevertheless, it is seven orders of magnitude lower than that of $[Gd(DOTA)(H_2O)]^{-}$, a clinically used MRI contrast agent.

Table 2. Formal potentials $E_{1/2}$ of Eu^{III}/Eu^{II} complexes, thermodynamic stability constants of Eu^{II} ($\lg K_{Eu^{II}}$), Sr^{II} ($\lg K^{Sr}$), and Gd^{III} ($\lg K^{Gd}$) complexes ($I = 0.1$ M $(CH_3)_4NCl$; 25 °C).

Ligand	$E_{1/2}$ [mV] versus Ag/AgCl	Ref.	$\lg K_{Eu^{II}}$	Ref.	$\lg K^{Sr}$	Ref.	$\lg K^{Gd}$	Ref.
H_2O	−585	this work						
DTPA	−1340[a]	[8]	10.08[b]	[26a]	9.68	[26b]	22.46	[26b]
ODDA	−820	[9]	9.85	[9]	8.66	[9]	11.93	[27a]
ODDM	−920	[9]	13.07	[9]	11.34	[9]	15.51[f]	[27b]
2.2.2	−205[a]	[21]	10.5	[21]	8.26	[25]	–	–
DOTA	−1135	this work	16.75 ± 0.07[c]/16.91[d]	this work	14.38[e]	[22a]	24.0[e]	[22b]
TETA	−996	this work	7.02 ± 0.05[c]/7.06[d]	this work	5.91[e]	[22a]	13.77[e]	[22b]

[a] Measured versus SCE. [b] In 1 M KCl. [c] Determined by pH potentiometry. [d] Calculated value from Equation (1). [e] In 0.1 M KCl. [f] In 0.16 M NaCl.

  0947-6539/03/0906-1397 $ 20.00+.50/0

^{17}O NMR, NMRD, and EPR measurements: A variable-temperature and multiple-field oxygen-17 and proton relaxation study, complemented with EPR measurements, was performed on $[Eu^{II}(DOTA)(H_2O)]^{2-}$ and $[Eu^{II}(TETA)]^{2-}$ in aqueous solution with the objective of determining parameters that describe water exchange, rotation, electronic relaxation, and proton relaxivity. Oxygen-17 chemical shifts $\Delta\omega_r$, longitudinal ($1/T_{1r}$) and transverse ($1/T_{2r}$) relaxation rates, longitudinal proton relaxivities r_1 and EPR peak-to-peak linewidths were measured and then analyzed simultaneously.[9] All equations used are given in the Appendix. The number of inner-sphere water molecules q the Eu^{II} complex in solution was assumed to be the same as determined in the solid state for the Sr^{II} analogues, that is, $q=1$ for $[Eu^{II}(DOTA)(H_2O)]^{2-}$ and $q=0$ for $[Eu^{II}(TETA)]^{2-}$. The ^{17}O NMR and NMRD data in both cases support this assumption. For $[Eu^{II}(TETA)]^{2-}$, the $1/T_{1r}$ and $1/T_{2r}$ values are equal within the experimental error, and the $\Delta\omega_r$ values are about 10–20% of those measured for $[Eu^{II}(DOTA)(H_2O)]^{2-}$, which indicates only outer-sphere contributions to the chemical shift (experimental data in Supporting Information). Hence, for $[Eu^{II}(TETA)]^{2-}$ the experimental NMRD and EPR data were fitted to Equations (13)–(15) and (21)–(23) by assuming only outer-sphere proton relaxation, and the parameters describing electronic relaxation and diffusion were thus obtained. The experimental data and the fitted curves are presented in Figures 4 and 5, and the parameters obtained are given in Table 3.

Water exchange on $[Eu^{II}(DOTA)(H_2O)]^{2-}$: Based on the ^{17}O chemical shifts, a value of $A/\hbar = -3.3 \pm 0.3$ was calculated for the scalar coupling constant of $[Eu^{II}(DOTA)(H_2O)]^{2-}$. This was obtained without assuming any outer-sphere contribution ($C_{os}=0$), since due to the lack of a regime of slow water exchange in the temperature range studied, C_{os} could not be determined. Nevertheless, the outer-sphere mechanism can contribute up to 20% of the total chemical shift, as is known for Gd^{III} complexes[28] and also evidenced by the chemical shifts measured on $[Eu^{II}(TETA)]^{2-}$. By fixing C_{os} to 0.2 in the fit, $A/\hbar = -3.16 \pm 0.08$ could be calculated. The quantity $A/\hbar$ characterizes electron delocalization from the Eu^{II} onto the ligand nucleus, and hence the low $A/\hbar$ value of $[Eu^{II}(DOTA)(H_2O)]^{2-}$ in comparison with other Eu^{II} complexes (Table 3) implies a weaker interaction between the metal ion and the water oxygen atom. This is in perfect agreement with the longer $M-O_{water}$ bond length.

The transverse ^{17}O relaxation rates $1/T_{2r}$ lie in the fast exchange region and thus are determined by the relaxation rate of the coordinated water molecule $1/T_{2m}$, which itself is influenced by the water residence time $\tau_m = 1/k_{ex}$, the longitudinal electronic relaxation rate $1/T_{1e}$, and the nuclear hyperfine coupling constant $A/\hbar$ [Eq. (10)]. The water exchange rate k_{ex}^{298} on $[Eu^{II}(DOTA)(H_2O)]^{2-}$ is one order of magnitude higher than on the 18-membered macrocyclic $[Eu^{II}(ODDA)(H_2O)]$ or macrobicyclic $[Eu^{II}(2.2.2)(H_2O)_2]^{2+}$, and it is the highest among all Eu^{II} complexes,[8–10] albeit lower than on the aqua ion (Table 3). The pressure dependence of the transverse ^{17}O relaxation rates gives access to the water-exchange mechanism. The experimental data for $[Eu^{II}(DOTA)(H_2O)]^{2-}$ were fitted to Equation (16) (Figure 6). The almost zero activation volume ($\Delta V^{\neq} = +0.1 \pm 1.0\ cm^3 mol^{-1}$) indicates an interchange (I) water exchange

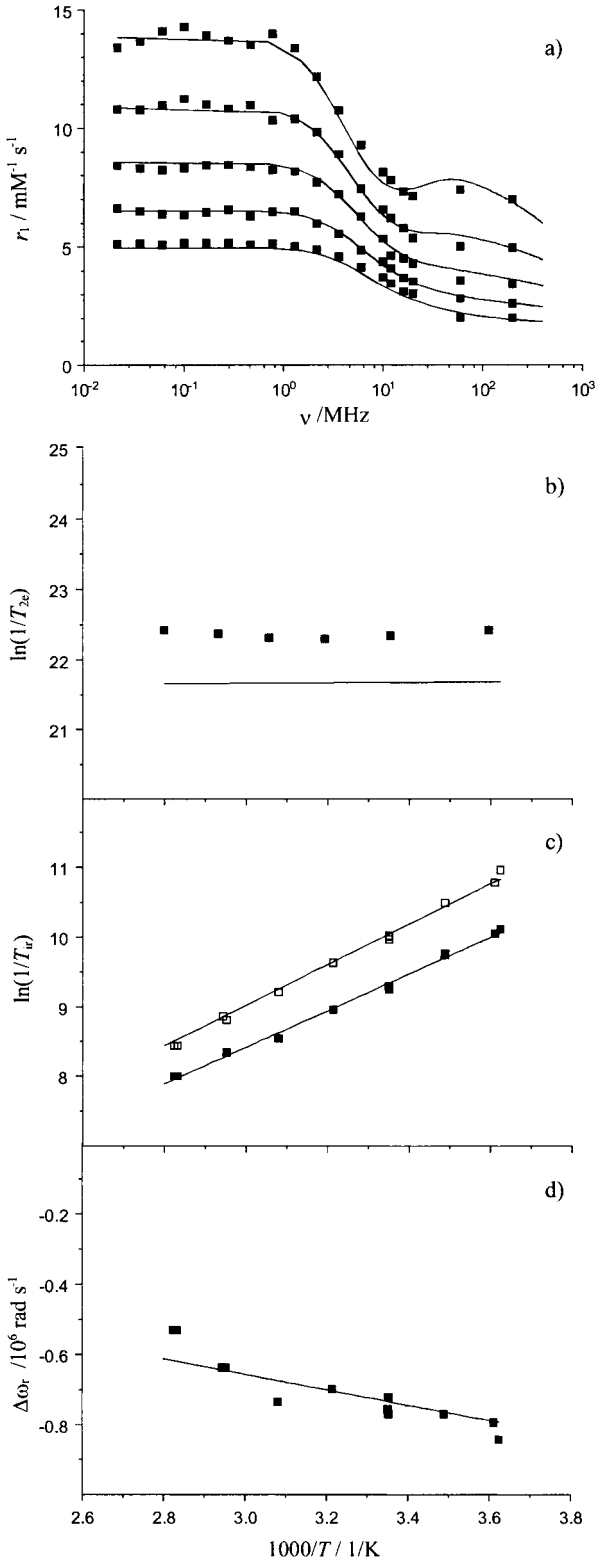

Figure 4. a) ^{1}H NMRD profiles at 5, 15, 25, 37, and 50 °C (from top to bottom). b) Temperature dependence of transverse electronic relaxation rates at 0.34 T. c) Longitudinal (filled squares) and transverse (empty squares) ^{17}O relaxation rates. d) ^{17}O chemical shifts at 9.4 T of $[Eu^{II}(DOTA)(H_2O)]^{2-}$ in solution.

0947-6539/03/0906-1398 $ 20.00+.50/0 *Chem. Eur. J.* **2003**, *9*, No. 6

Table 3. Parameters obtained from the simultaneous fit of variable-temperature ^{17}O relaxation rates, chemical shifts, and ^{1}H NMRD and EPR data.

	$[Eu^{II}(H_2O)_8]^{2+}$[a]	$[Eu^{II}(DTPA)(H_2O)]^{3-}$[b]	$[Eu^{II}(ODDA)(H_2O)]$[c]	$[Eu^{II}(2.2.2)(H_2O)_2]^{3+}$[d]	$[Eu^{II}(DOTA)(H_2O)]^{2-}$	$[Eu^{II}(TETA)]^{2-}$
k_{ex}^{298} [$10^9 s^{-1}$]	4.4	1.3	0.43	0.31	2.46 ± 0.5	
ΔH^{+} [$kJ\,mol^{-1}$]	15.7	26.3	22.5	30.6	21.4 ± 2.0	
ΔS^{+} [$J\,mol^{-1}\,K^{-1}$]	−7.0	+18.4	-4.0	+20.5	$+6.9 \pm 0.4$	
ΔV^{+} [$cm^3\,mol^{-1}$]	−11.3	+4.5	−3.9	+0.9	$+0.1 \pm 0.1$[e]	
$A/\hbar$ [$10^6\,rad\,s^{-1}$]	−3.7	−3.5	−4.3	−4.1	-3.3 ± 0.3	
τ_r^{298} [ps]	16.3	74	58.2	90.3[f]	123 ± 10[f]	
E_R [$kJ\,mol^{-1}$]	21.3	18.9	23.9	17.9	22.3 ± 2.3	
τ_v^{298} [ps]	1.0	13.6	14.3	17.0	22.7 ± 1.7	17.9 ± 1.4
E_v [$kJ\,mol^{-1}$]	12.5	1[g]	1[g]	1[g]	1[g]	1[g]
Δ^2 [$10^{20} s^{-2}$]	1.13	1.7	1.01	0.21	0.20 ± 0.02	0.73 ± 0.06
D_{EuH}^{298} [$10^{-10} m^2 s^{-1}$]	22.9	23	24.3	15.7	15.2 ± 1.0	18.4 ± 0.4
E_{DeuH} [$kJ\,mol^{-1}$]	20.1	29	25.4	36.3	30.2 ± 0.9	22.5 ± 0.7

[a] Ref. [7]. [b] Ref. [8], fit without EPR data. [c] Ref. [9], fit without EPR data. [d] Ref. [10]. [e] The error in ΔV^{+} is usually considered to be $\pm 1\ cm^3\,mol^{-1}$ or 10% of the ΔV^{+} value, whichever is largest, to take into account possible effects of nonrandom errors. [f] τ_{RO}^{298}. [g] Value fixed in the fit.

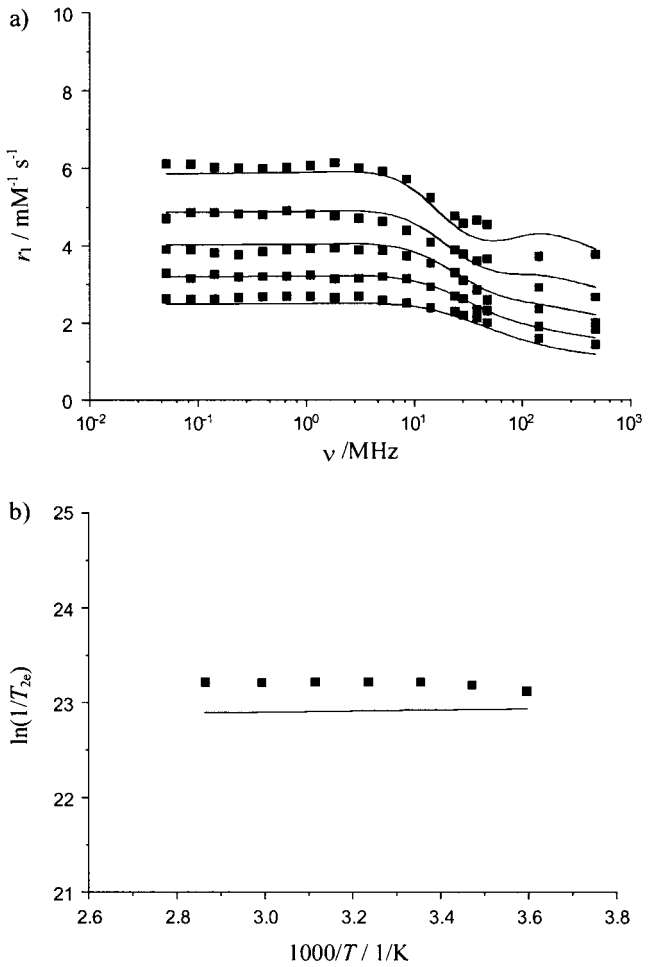

Figure 5. a) ^{1}H NMRD profiles at 5, 15, 25, 37, and 50 °C (from top to bottom). b) Temperature dependence of transverse electronic relaxation rates at 0.34 T of $[Eu^{II}(TETA)]^{2-}$ in solution.

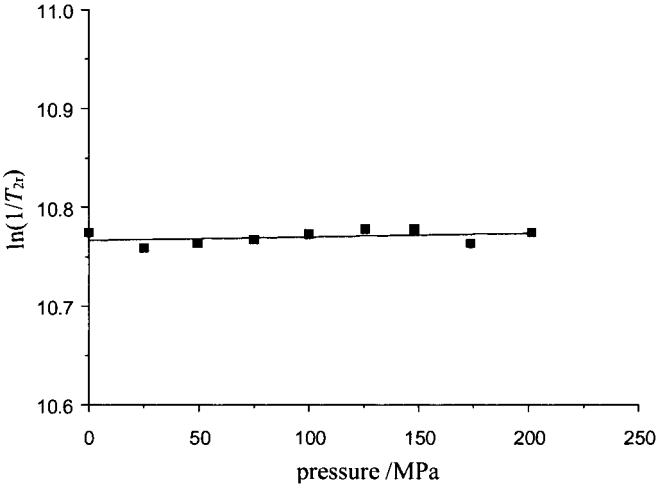

Figure 6. Pressure dependence of the reduced transverse ^{17}O relaxation rates at $B = 9.4$ T and 3 °C for $[Eu^{II}(DOTA)(H_2O)]^{2-}$.

mechanism. In comparison to Gd^{III} complexes, the Eu^{II} analogues have 2–3 orders of magnitude faster water exchange, which generally proceeds by a less dissociative mechanism. For instance, for $[Gd(DOTA)(H_2O)]^{-}$ the activation volume $\Delta V^{+} = +10.5\ cm^3\,mol^{-1}$ points to an almost limiting dissociative (D) mechanism.[5, 29] There are multiple reasons for this shift in the water exchange mechanism from dissociative for $Gd^{III}L$ towards less dissociative or even associative for $Eu^{II}L$ complexes. In addition to the larger ionic size and smaller charge (lower charge density) of divalent Eu^{II}, the longer Eu^{II}–O_{water} distance is another significant factor. In the $DOTA^{4-}$ complex, the Eu^{II}–O_{water} distance is particularly elongated (2.85 versus 2.41 Å in $[Gd(DOTA)(H_2O)]^{-}$).[15] This long distance allows a second water molecule to enter the coordination sphere parallel with the departure of the loosely coordinated leaving water molecule in the case of $[Eu^{II}(DOTA)(H_2O)]^{2-}$, as was experimentally proved by the near-zero activation volume (i.e., I mechanism). The approach of the incoming water molecule facilitates the departure of the coordinated water molecule and accelerates the exchange process. Interestingly, an interchange water exchange mechanism, but with an exchange rate one order of magnitude lower ($k_{ex}^{298} = 0.31 \times 10^9\ s^{-1}$) was determined for $[Eu^{II}(2.2.2)(H_2O)_2]^{2+}$.[10] In this cryptate, the metal ion is ten-coordinate, in contrast to the nine-coordinate $[Eu^{II}(DOTA)(H_2O)]^{2-}$. Therefore the interchange mechanism here means the entrance of a third water molecule (eleventh donor atom) into the coordination sphere of Eu^{II}, which requires more energy than the entrance of a second water molecule (tenth coordinating atom) in $[Eu^{II}(DOTA)(H_2O)]^{2-}$. In addition, the considerably shorter

$M-O_{water}$ distance in $[Eu^{II}(2.2.2)(H_2O)_2]^{2+}$ indicates stronger binding.

Rotation: The rotational correlation time τ_R also has a determining role in proton relaxivity, and for low molecular weight complexes it is usually a limiting factor. Information on τ_R is obtained from the longitudinal ^1H and ^{17}O relaxation rates, which are related to rotation of the $Eu^{II}-H_{water}$ and $Eu^{II}-O_{water}$ vectors, respectively. Recently, it was found for $[Gd(DOTA)(H_2O)]^-$ that τ_R of the $Gd^{III}-H_{water}$ vector is about 65% of the overall correlation time of the complex, which itself is close to τ_R of the $Gd^{III}-O_{water}$ vector.[30] In our analysis we also separated the rotational correlation times of the $M-O_{water}$ and the $M-H_{water}$ vectors [τ_{RO} and τ_{RH}; Eqs. (8) and (20)]. Two parameters were fitted: τ_{RO}, regarded as a true rotational correlation time of the complex, and the τ_{RH}/τ_{RO} ratio. For the distance r_{EuO} in $[Eu^{II}(DOTA)(H_2O)]^{2-}$ the solid-state value of the corresponding Sr^{II} complex was used, and the distance r_{EuH} was estimated to be 3.50 Å.[7] The calculated τ_{RH}/τ_{RO} ratio is 0.54 ± 0.13, similar to that of $[Gd(DOTA)(H_2O)]^-$ (0.65 ± 0.2).[30] For $[Eu^{II}(DOTA)(H_2O)]^{2-}$ there is no experimentally determined quadrupolar coupling constant for the bound oxygen atom of water [χ in Eq. (7)], in contrast to $[Ln^{III}(DOTAM)(H_2O)]^{3+}$ complexes, for which $\chi(1+\eta^2/3)^{1/2} = 5.2$ MHz was obtained (DOTAM = DOTA tetraamide).[30] Eu^{II} has a lower charge density than the lanthanide(III) ions and, moreover, the $M-O_{water}$ distance is considerably longer than in $[Ln^{III}(DOTAM)(H_2O)]^{3+}$ complexes, so it seemed more reasonable in the present study to use the value for pure water of $\chi(1+\eta^2/3)^{1/2} = 7.58$ MHz. The rotational correlation times obtained for $[Eu^{II}(DOTA)(H_2O)]^{2-}$ ($\tau_{RO}^{298} = 123$ ps and $\tau_{RH}^{298} = 66$ ps) are typical values for a low molecular weight complex and are comparable to those of other Eu^{II} complexes.

Electronic relaxation: The transverse electronic relaxation rates $1/T_{2e}$ were measured experimentally by EPR spectroscopy, while the longitudinal relaxation rates $1/T_{1e}$ were calculated from the $1/T_{2e}$ values by using Equations (13)–(15). Additionally, the NMRD data also contain information on electronic relaxation. The EPR spectrum of Eu^{II} is the superposition of 12 lines originating from coupling to two isotopes, ^{151}Eu and ^{153}Eu, which have the same spin ($I = 5/2$) and similar natural abundance (47.82 and 52.18%, respectively). This isotropic hyperfine structure becomes more visible at high frequency (Figure 7), where the lines are narrower (< 20–30 G). The analysis of the EPR spectra led to a coupling constant of around 36 G for $[Eu^{II}(DOTA)(H_2O)]^{2-}$, a similar value to that calculated for $Eu^{II}(aq)$.[7] For Gd^{III} complexes, the new Rast–Borel approach, which also involves static zero-field splitting, has contributed much to the understanding of electron spin relaxation.[31] The extension of this theory to Eu^{II} is currently in progress but has not yet achieved. Therefore, in the present study, we used the traditional Solomon–Bloembergen–Morgan analysis, and only a transient zero-field splitting (ZFS) mechanism was considered. This is characterized by the trace of the square of the zero-field splitting tensor Δ^2 and the correlation time for the modulation of the ZFS τ_v as fitted

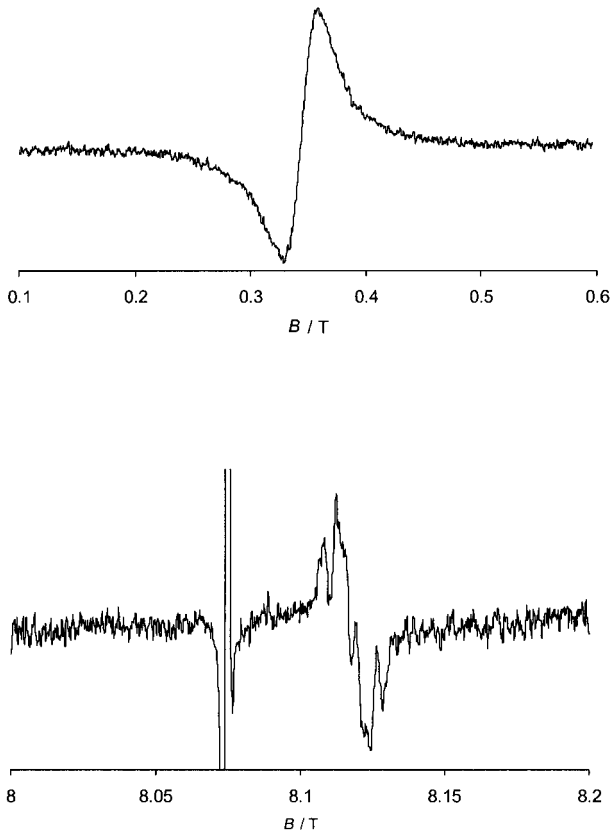

Figure 7. X band (top) and 225 GHz EPR (bottom) spectra of $[Eu^{II}(DOTA)(H_2O)]^{2-}$ at 25 °C. Signal at 8.07 T corresponds to the BDPA reference.

parameters.[32] However, the quality of fit of the X-band EPR data for both $[Eu^{II}(DOTA)(H_2O)]^{2-}$ and $[Eu^{II}(TETA)]^{2-}$ (Figures 4 and 5) evidences the imperfection of the present theory (the analysis of the EPR spectra recorded at 75 and 225 GHz, 2.7 and 8.1 T, was not possible with the current approach and hence will be reported later using the improved theory). Nevertheless, the peak-to-peak EPR linewidths, obtained by deconvolution of the spectra to 12 lines to take into account the hyperfine coupling, give a direct experimental proof of a remarkable variation in rate of electron spin relaxation in the series of Eu^{II} complexes studied. The linewidth (X band, 298 K) is greater than 1000 G for $[Eu^{II}(DTPA)(H_2O)]^{3-}$, 763 G for $[Eu^{II}(TETA)]^{2-}$, 317 G for $[Eu^{II}(DOTA)(H_2O)]^{2-}$, 135 G for $[Eu^{II}(2.2.2)(H_2O)_2]^{2+}$, and 84 G for $Eu^{II}(aq)$. Interestingly, the same pattern, that is, much faster electronic relaxation of the TETA complex in comparison to the DOTA complex was found for Gd^{III}.[33]

Proton relaxivity: The longitudinal water proton relaxation rates were measured at variable temperature and multiple fields, and then normalized to 1 mM concentration to obtain the relaxivity r_1. The relaxivity curves of $[Eu^{II}(DOTA)(H_2O)]^{2-}$ are typical of low molecular weight complexes with one inner-sphere water molecule, whereas those of $[Eu^{II}(TETA)]^{2-}$ are much lower and represent only the outer-sphere contribution (e.g., $r_1 = 2.60\ mM^{-1}s^{-1}$ for $[Eu^{II}(TETA)]^{2-}$ vs $4.32\ mM^{-1}s^{-1}$ for $[Eu^{II}(DOTA)(H_2O)]^{2-}$; 298 K, 20 MHz). Remarkably, $[Eu^{II}(DOTA)(H_2O)]^{2-}$ has a

0947-6539/03/0906-1400 $ 20.00+.50/0 *Chem. Eur. J.* **2003**, *9*, No. 6

25% higher relaxivity at 298 K and 20 MHz than $[Eu^{II}(DTPA)(H_2O)]^{3-}$ (3.49 $mM^{-1}s^{-1}$), and it is very close to r_1 of $[Gd^{III}(DOTA)(H_2O)]^{-}$ (4.74 $mM^{-1}s^{-1}$). The electron spin relaxation in the DTPA complex is the fastest among all Eu^{II} chelates, and it is fast enough to limit proton relaxivity at 20 MHz. This phenomenon has never been observed for Gd^{III} complexes, not even for macromolecular ones such as dendrimers, in which the large number of gadolinium ions in a close proximity usually increases the rate of electron spin relaxation by an additional dipole–dipole coupling mechanism.[34] Electron spin relaxation in $[Eu^{II}(DOTA)(H_2O)]^{2-}$ is much slower than in $[Eu^{II}(DTPA)(H_2O)]^{3-}$, probably due to the higher symmetry of the complex, and does not limit proton relaxivity. Therefore, the relaxivity of $[Eu^{II}(DOTA)(H_2O)]^{2-}$ is exclusively limited by rotation, like that of $[Gd(DOTA)(H_2O)]^{-}$, which explains the similar values.

The next step towards potential Eu^{II}-based pO_2-responsive MRI contrast agents will be the synthesis of macromolecules to optimize (slow down) rotation and thus increase proton relaxivity. A good chelator for attachment to macromolecules must ensure sufficient control of the reduced Eu^{II} state, and the complex must have optimal rates of water exchange and electronic relaxation. The water exchange rate on $[Eu^{II}(DOTA)(H_2O)]^{2-}$ is about one order of magnitude higher than the optimal value ($k_{ex,opt} \approx 10^8\,s^{-1}$) for attaining maximum proton relaxivity. The complex that fulfils most of these criteria is $[Eu^{II}(2.2.2)(H_2O)_2]^{2+}$. This cryptate has several beneficial features: high redox stability, two inner-sphere water molecules to allow for increased proton relaxivity, optimal water exchange rate, and slow electron spin relaxation.[10]

Appendix

Oxygen-17 NMR spectroscopy: From the measured ^{17}O NMR relaxation rates and angular frequencies of the paramagnetic solutions ($1/T_1$, $1/T_2$, and ω), and of the reference ($1/T_{1A}$, $1/T_{2A}$, and ω_A) one can calculate the reduced relaxation rates and chemical shift, $1/T_{1r}$, $1/T_{2r}$, and ω_r, which may be written as in Equations (2)–(4), where P_m is the molar fraction of bound water, $1/T_{1m}$ and $1/T_{2m}$ are the relaxation rates of the bound water and ω_m is the chemical shift difference between bound and bulk water.

$$\frac{1}{T_{1r}} = \frac{1}{P_m}\left[\frac{1}{T_1} - \frac{1}{T_{1A}}\right] = \frac{1}{T_{1m} + \tau_m} \tag{2}$$

$$\frac{1}{T_{2r}} = \frac{1}{P_m}\left[\frac{1}{T_2} - \frac{1}{T_{2A}}\right] = \frac{1}{\tau_m}\frac{T_{2m}^{-2} + \tau_m^{-1}T_{2m}^{-1} + \Delta\omega_m^2}{(\tau_m^{-1} + T_{2m}^{-1})^2 + \Delta\omega_m^2} \tag{3}$$

$$\Delta\omega_r = \frac{1}{P_m}(\omega - \omega_A) = \frac{\Delta\omega_m}{(1 + \tau_m T_{2m}^{-1})^2 + \tau_m^2\Delta\omega_m^2} + \Delta\omega_{os} \tag{4}$$

$\Delta\omega_m$ is determined by the hyperfine or scalar coupling constant $A/\hbar$ according to Equation (5), where B is the magnetic field, S is the electron spin, and g_L is the isotropic Landé g factor.

$$\Delta\omega_m = \frac{g_L\mu_B S(S+1)B}{3k_B T}\frac{A}{\hbar} \tag{5}$$

The outer-sphere contribution to the chemical shift is assumed to be linearly related to $\Delta\omega_m$ by a constant C_{os} [Eq. (6)].

$$\Delta\omega_{os} = C_{os}\,\Delta\omega_m \tag{6}$$

The ^{17}O longitudinal relaxation rates are given by Equation (7) (see also Equation (8)), where γ_S is the electron and γ_I is the nuclear gyromagnetic ratio ($\gamma_S = 1.76 \times 10^{11}\,rad\,s^{-1}\,T^{-1}$, $\gamma_I = -3.626 \times 10^7\,rad\,s^{-1}\,T^{-1}$), r is the effective distance between the electron charge and the ^{17}O nucleus, I is the nuclear spin (5/2 for ^{17}O), χ is the quadrupolar coupling constant, and η is an asymmetry parameter.

$$\frac{1}{T_{1m}} = \left[\frac{1}{15}\left(\frac{\mu_0}{4\pi}\right)^2\frac{\hbar^2\gamma_I^2\gamma_S^2}{r_{EuO}^6}S(S+1)\right]\times\left[6\tau_{d1} + 14\frac{\tau_{d2}}{1+\omega_S^2\tau_{d2}^2}\right] + \frac{3\pi^2}{10}\frac{2I+3}{I^2(2I-1)}\chi^2(1+\eta^2/3)\tau_{RO} \tag{7}$$

where:

$$\frac{1}{\tau_{di}} = \frac{1}{\tau_m} + \frac{1}{\tau_{RO}} + \frac{1}{T_{ie}} \qquad i = 1, 2 \tag{8}$$

The overall rotational correlation time τ_{RO} is assumed to have a simple exponential temperature dependence with an activation energy E_R [Eq. (9)].

$$\tau_{RO} = \tau_{RO}^{298}\exp\left\{\frac{E_R}{R}\left(\frac{1}{T} - \frac{1}{298.15}\right)\right\} \tag{9}$$

In the transverse relaxation the scalar contribution $1/T_{2sc}$ is the most important [Eq. (10)], where $1/\tau_{s1}$ is the sum of the exchange rate constant and the electron spin relaxation rate [Eq. (11)].

$$\frac{1}{T_{2m}} \cong \frac{1}{T_{2sc}} = \frac{S(S+1)}{3}\left(\frac{A}{\hbar}\right)^2\tau_{s1} \tag{10}$$

where:

$$\frac{1}{\tau_{s1}} = \frac{1}{\tau_m} + \frac{1}{T_{1e}} \tag{11}$$

The inverse binding time (or exchange rate k_{ex}) of water molecules in the inner sphere is assumed to obey the Eyring equation [Eq. (12)], where $\Delta S^{\ddagger}$ and $\Delta H^{\ddagger}$ are the entropy and enthalpy of activation for the exchange process, and k_{ex}^{298} is the exchange rate at 298.15 K.

$$\frac{1}{\tau_m} = k_{ex} = \frac{k_B T}{h}\exp\left\{\frac{\Delta S^{\ddagger}}{R} - \frac{\Delta H^{\ddagger}}{RT}\right\} = \frac{k_{ex}^{298}T}{298.15}\exp\left\{\frac{\Delta H^{\ddagger}}{R}\left(\frac{1}{298.15} - \frac{1}{T}\right)\right\} \tag{12}$$

The electron spin relaxation rates $1/T_{1e}$ and $1/T_{2e}$ for metal ions in solution with $S > 1/2$ are mainly governed by a transient zero-field splitting (ZFS) mechanism.[31] The ZFS terms can be expressed by Equations (13) and (14), where Δ^2 is the trace of the square of the transient zero-field splitting

tensor, τ_v is the correlation time [Eq. (15)] for the modulation of the ZFS with the activation energy E_v, and ω_s is the Larmor frequency of the electron spin.

$$\left(\frac{1}{T_{1e}}\right)^{ZFS} = \frac{1}{25}\Delta^2\tau_v\{4S(S+1)-3\}\left(\frac{1}{1+\omega_S^2\tau_v^2}+\frac{4}{1+4\omega_S^2\tau_v^2}\right) \quad (13)$$

$$\left(\frac{1}{T_{2e}}\right)^{ZFS} = \Delta^2\tau_v\left[\frac{5.26}{1+0.372\omega_S^2\tau_v^2}+\frac{7.18}{1+1.24\omega_S\tau_v}\right] \quad (14)$$

$$\tau_v = \tau_v^{298}\exp\left\{\frac{E_v}{R}\left(\frac{1}{T}-\frac{1}{298.15}\right)\right\} \quad (15)$$

The pressure dependence of $\ln k_{ex}$ is linear [Eq. (16)], where $\Delta V^{\ddagger}$ is the activation volume and $(k_{ex})_0^T$ is the water exchange rate at zero pressure and temperature T.

$$\frac{1}{\tau_m} = k_{ex} = (k_{ex})_0^T\exp\left\{-\frac{\Delta V^{\ddagger}}{RT}P\right\} \quad (16)$$

NMRD: The measured proton relaxivities (normalized to 1 mM Eu^{II} concentration) contain both inner- and outer-sphere contributions [Eq. (17)].

$$r_1 = r_{1is} + r_{1os} \quad (17)$$

The inner-sphere term is given by Equation (18), where q is the number of inner-sphere water molecules.

$$r_{1is} = \frac{1}{1000}\times\frac{q}{55.55}\times\frac{1}{T_{1m}^H+\tau_m} \quad (18)$$

The longitudinal relaxation rate of inner sphere protons, $1/T_{1m}^H$ can be expressed by Equation (19), where r_{EuH} is the effective distance between the Eu^{II} electron spin and the water protons, ω_I is the proton resonance frequency, and τ_{diH} is given by Equation (20), where τ_{RH} is the rotational correlation time of the Eu^{II}–H_{water} vector.

$$\frac{1}{T_{1m}^H} = \frac{2}{15}\left(\frac{\mu_o}{4\pi}\right)^2\frac{\hbar^2\gamma_S^2\gamma_I^2}{r_{EuH}^6}S(S+1)\left[\frac{3\tau_{d1H}}{1+\omega_I^2\tau_{d1H}^2}+\frac{7\tau_{d2H}}{1+\omega_S^2\tau_{d2H}^2}\right] \quad (19)$$

$$\frac{1}{\tau_{diH}} = \frac{1}{\tau_m}+\frac{1}{\tau_{RH}}+\frac{1}{T_{ie}} \qquad i=1,2 \quad (20)$$

The outer-sphere contribution can be described by Equation (21), where N_A is the Avogadro constant, and J_{os} is a spectral density function [Eq. (22)].

$$r_{1os} = \frac{32N_A\pi}{405}\left(\frac{\mu_0}{4\pi}\right)^2\frac{\hbar^2\gamma_S^2\gamma_I^2}{a_{EuH}D_{EuH}}S(S+1)[3J_{os}(\omega_I,T_{1e})+7J_{os}(\omega_S,T_{2e})] \quad (21)$$

$$J_{os}(\omega,T_{je}) = Re\left[\frac{1+\frac{1}{4}\left(i\omega\tau_{EuH}+\frac{\tau_{EuH}}{T_{je}}\right)^{1/2}}{1+\left(i\omega\tau_{EuH}+\frac{\tau_{EuH}}{T_{je}}\right)^{1/2}+\frac{4}{9}\left(i\omega\tau_{EuH}+\frac{\tau_{EuH}}{T_{je}}\right)+\frac{1}{9}\left(i\omega\tau_{EuH}+\frac{\tau_{EuH}}{T_{je}}\right)^{3/2}}\right] \quad (22)$$

$$j=1,2$$

For the temperature dependence of the diffusion coefficient D_{EuH} for the diffusion of a water proton away from a Eu^{II} complex, we assume a exponential temperature dependence, with an activation energy E_{DEuH} [Eq. (23)].

$$D_{EuH} = D_{EuH}^{298}\exp\left\{\frac{E_{DEuH}}{R}\left(\frac{1}{T}-\frac{1}{298.15}\right)\right\} \quad (23)$$

Conclusion

The redox stability of the Eu^{II} complexes formed with the 12-membered $DOTA^{4-}$ and 14-membered $TETA^{4-}$ macrocycles is inferior to that of 18-membered macrocyclic Eu^{II} chelates. The thermodynamic complex stability constants calculated from the formal electrode potentials agree well with those measured by pH potentiometry. In comparison to the Sr^{II} analogues, Eu^{II} complexes have about two orders of magnitude higher thermodynamic stability constants, $[Eu^{II}(DOTA)(H_2O)]^{2-}$ being the most stable among all Eu^{II} complexes reported so far ($\log K_{Eu^{II}} = 16.75$). Solid-state structures of the corresponding Sr^{II} chelates revealed no inner-sphere water in the TETA, and one water molecule in the DOTA complex, in contrast to previous MD simulations. This hydration pattern is retained in solution, as the ^{17}O NMR and NMRD data showed for the Eu^{II} analogues. $[Eu^{II}(DOTA)(H_2O)]^{2-}$ has very fast water exchange ($k_{ex}^{298} = 2.46\times10^9\,s^{-1}$). This was explained in terms of a long $M-O_{water}$ distance, which, together with the low charge density of the divalent Eu^{II} ion, results in an interchange water exchange mechanism.

Experimental Section

H_4TETA was purchased from Fluka, and H_4DOTA was kindly provided by Guerbet GCA and used without further purification. The concentration of ligand solutions was determined from the pH-potentiometric titration curves obtained in the absence and presence of a 50-fold excess of $CaCl_2$. In this method, the difference of the inflection points of the two titration curves corresponds to two ligand equivalents. For the preparation of $Eu(O_3SCF_3)_3$ and $EuCl_3$ solutions, we used the salts of the highest analytical grade (Fluka and Alfa Aesar). The concentration of the solutions was determined by complexometric titrations with standardized $Na_2(H_2EDTA)$ and xylenol orange indicator at pH 5.6–6.0 in hexamethylenetetraamine buffer. The solutions of the Eu^{III} complexes were prepared by mixing appropriate quantities of the ligand and the metal (3–5% ligand excess) and setting the pH with NaOH. The solutions of $[Eu^{II}(DOTA)(H_2O)]^{2-}$ and $[Eu^{II}(TETA)]^{2-}$ were prepared by reducing the corresponding Eu^{III} complexes with controlled coulometry in a home-built electrolysis cell by using an EG&G 263A galvanostat/potentiostat.[8] The reduction potential used was 0.4–0.5 V lower than the $E_{1/2}$ calculated from the cyclovoltammogram of the $Eu^{III}L$ solution ($L = DOTA^{4-}$ and $TETA^{4-}$). The cyclovoltammetry curves were recorded on the same EG&G 263A galvanostat/potentiostat apparatus with a standard cell in EuL solution ($c_{EuL} = 0.004$ M and 0.1 M NaCl as supporting electrolyte) with a glassy carbon microelectrode and an Ag/AgCl in 3 M NaCl reference electrode at 50 mV s^{-1} scan rate.

After reduction, the yellow $[Eu^{II}(DOTA)(H_2O)]^{2-}$ and orange $[Eu^{II}(TETA)]^{2-}$ solutions were kept at −20 °C until used to avoid oxidation. The UV/Vis spectra of the solutions were recorded on a Perkin-Elmer Lambda 5 spectrophotometer in a special 1 mm cuvette suitable for use under anaerobic conditions. The spectra are deposited in the Supporting Information.

0947-6539/03/0906-1402 $ 20.00+.50/0 *Chem. Eur. J.* **2003**, *9*, No. 6

The concentration of the Eu^{II} samples prepared by electrolysis was determined by Zimmermann–Reinhardt redox titration with a tenfold excess of $Fe_2(SO_4)_3$ in H_2SO_4/H_3PO_4 solution (4 M), then the quantity Fe^{II} produced, corresponding to the amount of Eu^{II}, was titrated with a $K_2Cr_2O_7$ solution. The poly(amino carboxylate) ligands showed no interference with the $K_2Cr_2O_7$ solution. The redox potential of the titrated solution was monitored with a combined Pt redox electrode (reference electrode part 3 M KCl, Ag/AgCl, Metrohm) connected to a Metrohm 692 pH/ion meter. The concentration determined in this way corresponded well, within the limit of the precision of the titration, to the Eu^{III} quantity weighed in. All Eu^{II} samples were manipulated under nitrogen atmosphere with rigorous exclusion of oxygen.

Equilibrium studies: The complex stability constants were determined by pH potentiometry at constant ionic strength (0.1 M $(CH_3)_4NCl$). The titrations were carried out in a thermostatically controlled vessel (25.0 ± 0.2 °C), and the $(CH_3)_4NOH$ titrant solution was dosed with a Metrohm Dosimat 665 automatic burette and a combined glass electrode (C14/02-SC, reference electrode part Ag/AgCl in 3 M KCl, Moeller Scientific Glass Instruments, Switzerland) connected to a Metrohm 692 pH/ion meter. The titrated solution (3–4 mL) was stirred with a magnetic stirrer and bubbled with a constant N_2 flow to avoid the effects of O_2 and CO_2. Stability constants were determined in 0.002–0.003 M solutions from 3–4 parallel titrations, each curve containing 30–40 volume/pH data pairs in the pH range 2–10. Freshly reduced $EuCl_2$ solution was added to the previously deoxygenated sample solution and titrated immediately. The hydrogen ion concentration was calculated from the measured pH values, as suggested by Irving, by using a correction term, obtained as the difference between the measured and calculated pH values in a titration of HCl (0.01 M) with standardized $(CH_3)_4NOH$.[35]

^{17}O NMR measurements: For the variable-temperature studies, the $[Eu^{II}(DOTA)(H_2O)]^{2-}$ ($c = 0.0769$ mol kg^{-1}, pH 9.6) and $[Eu^{II}(TETA)]^{2-}$ ($c = 0.0607$ mol kg^{-1}, pH 10.5) solutions were filled with a syringe into glass spheres which were fitted into 10 mm NMR tubes. The NMR tubes containing the spheres had been previously closed with a septum in a glove box under nitrogen. Glass spheres are used to eliminate susceptibility effects.[36] The relaxation rates and chemical shifts were measured with respect to solutions of the corresponding Sr^{II} complex at similar concentrations and pH values as external reference. To improve the sensitivity in ^{17}O NMR, ^{17}O-enriched water (10% $H_2{}^{17}O$, Yeda (Israel)) was added to the solutions to yield in 1–2% ^{17}O enrichment. The ^{17}O NMR measurements were performed on a Bruker AM-400 spectrometer at 9.4 T, 54.2 MHz. Bulk-water longitudinal relaxation rates $1/T_1$ were obtained by the inversion recovery method,[37] and transverse relaxation rates $1/T_2$ by the Carr–Purcell–Meiboom–Gill spin echo technique.[38] Variable-pressure NMR spectra were recorded up to a pressure of 200 MPa on a Bruker AMX-400 spectrometer equipped with a home-made high-pressure probe.[39]

NMRD measurements: The $1/T_1$ nuclear magnetic relaxation dispersion (NMRD) profiles of the solvent protons at 5, 15, 25, 37, and 50 °C were obtained on 0.01 M $Eu^{II}L$ solutions on a Spinmaster FFC fast field cycling NMR relaxometer (Stelar), covering a continuum of magnetic fields from 5×10^{-4} to 0.47 T (corresponding to a proton Larmor frequency range of 0.022–20 MHz). Higher frequency measurements were performed on a 60 MHz electromagnet connected to an Avance-200 console and on a Bruker Avance-200 spectrometer.

EPR measurements: The X-band (9.425 GHz) spectra were recorded on a Bruker ESP 300E spectrometer. The spectra of $[Eu^{II}(DOTA)(H_2O)]^{2-}$ at higher frequencies were obtained on a home-built spectrometer (Department of Experimental Physics, Technical University of Budapest, Hungary). In this instrument a frequency-stabilized Gunn diode oscillator at 75 GHz base frequency is followed by a frequency tripler for 225 GHz measurements. A PTFE sample holder containing the aqueous samples is placed in an oversized waveguide so no resonant cavities are used. The transverse electronic relaxation rates $1/T_{2e}$ at various temperatures were obtained from the EPR line widths according to Reuben.[40] The concentrations of the samples were 0.01 M for the X-band experiments and 0.09 M for the higher frequencies.

Data analysis: The thermodynamic equilibrium constants were calculated by the program PSEQUAD.[41] The simultaneous least-squares fit of ^{17}O NMR, NMRD, and EPR data was performed with the program Scientist for

Table 4. Crystal data and structure refinement.

	$[C(NH_2)_3]_2[Sr(DOTA)(H_2O)]\cdot 4H_2O$	$[C(NH_2)_3]_2[Sr(TETA)]\cdot 5H_2O$
formula	$C_{18}H_{44}N_{10}O_{12}Sr$	$C_{20}H_{50}N_{10}O_{13}Sr$
M_r	680.25	726.32
temperature [K]	143(2)	143(2)
wavelength [Å]	0.71070	0.71070
crystal system	tetragonal	orthorhombic
space group	*P*4/*ncc*	$P2_12_12$
unit cell dimensions [Å]		
a [Å]	12.8200(10)	13.377(3)
b [Å]		13.676(2)
c [Å]	18.501(3)	8.947(3)
volume [Å^3]	3040.7(6)	1636.8(7)
Z	4	2
ρ_{calcd} [Mg cm^{-3}]	1.486	1.474
absorption coefficient [mm^{-1}]	1.844	1.720
F(000)	1424	764
crystal size [mm]	0.22 × 0.21 × 0.20	0.28 × 0.25 × 0.19
θ range for data collection [°]	2.25–24.40	2.28–24.40
index ranges	$-14 \le h \le 14$, $-14 \le k \le 14$, $-19 \le l \le 19$	$-15 \le h \le 15$, $-15 \le k \le 15$, $-10 \le l \le 10$
reflections collected	15713	8648
independent reflections	1187 [R(int) = 0.0506]	2526 [R(int) = 0.0366]
completeness to $\theta = 24.40°$	94.4%	99.2%
absorption correction	none	none
refinement method	full-matrix least-squares on F^2	full-matrix least-squares on F^2
data/restraints/parameters	1187/0/104	2526/9/221
final R indices [$I > 2\sigma(I)$][a]	$R1 = 0.0688$, $wR2 = 0.1566$	$R1 = 0.0317$, $wR2 = 0.0859$
R indices (all data)[a]	$R1 = 0.0734$, $wR2 = 0.1585$	$R1 = 0.0330$, $wR2 = 0.0865$
GOF[b]	1.183	1.128
extinction coefficient	0.027(2)	0.074(4)
largest diff. peak and hole [e Å^{-3}]	0.567, −1.050	0.442, −0.422

[a] $R = \Sigma\,||F_o| - |F_c||/\Sigma|F_o|$, $wR2 = \{\Sigma[w(F_o^2 - F_c^2)^2]/\Sigma[w(F_o^2)^2]\}^{1/2}$. [b] GOF $= \{\Sigma[wF_o^2 - F_c^2)^2]/(n-p)\}^{1/2}$, where n is the number of data and p is the number of parameters refined.

Windows by Micromath, version 2.0. The reported errors correspond to one standard deviation obtained by the statistical analysis.

X-ray measurements: For the preparation of crystals of $[C(NH_2)_3]_2[Sr(DOTA)]\cdot 4H_2O$, $H_4DOTA\cdot 3.5H_2O$ (116 mg, 0.248 mmol), $SrCO_3$ (35 mg, 0.237 mmol), and $[C(NH_2)_3]_2CO_3$ (45 mg, 0.242 mmol) were dissolved in water (0.5 mL). The solution was stirred and heated to 50 °C for a while. After the complete dissolution and CO_2 production the pH was set to 9.5 with NaOH, then the solution was filtered. After a few days of slow evaporation, one large colorless crystal had grown. This crystal was removed and dissolved in a quantity of water sufficient to produce a saturated solution after heating to 95 °C. Then the mixture was slowly cooled, and small crystals suitable for X-ray experiments were obtained.

To prepare crystals of $[C(NH_2)_3]_2[Sr(TETA)]\cdot 5H_2O$, $H_4TETA\cdot 4HCl\cdot 4H_2O$ (50 mg, 0.0775 mmol), $SrCO_3$ (11 mg, 0.0745 mmol), and $[C(NH_2)_3]_2CO_3$ (14 mg, 0.0777 mmol) were dissolved in water (0.5 mL). When the production of CO_2 finished, the pH was set to 10 with NaOH, then the solution was filtered, and part of the water was evaporated until the solution became oversaturated. After a few days of storage in refrigerator, small colorless plates were obtained and used for X-ray structural determination.

Data collection for $[C(NH_2)_3]_2[Sr(DOTA)(H_2O)]\cdot 4H_2O$ and $[C(NH_2)_3]_2[Sr(TETA)]\cdot 5H_2O$ was performed on a mar345 imaging plate detector system at 143 K, and data reduction was carried out with marHKL release 1.9.1.[42] Structure solution for all compounds was performed with ab initio direct methods. All structures were refined by full-matrix least-squares methods on F^2 with all non-H atoms anisotropically defined. H atoms were placed in calculated positions using the riding model with $U_{iso} = a^* U_{eq}(X)$ (where a is 1.5 for methyl hydrogen atoms and 1.2 for others, and X is the parent atom). Some water molecules in the complex $[C(NH_2)_3]_2[Sr(DOTA)(H_2O)]\cdot 4H_2O$ were disordered, and their occupancy factors were set to 0.5 for O4 and 0.25 for O5. In the case of $[C(NH_2)_3]_2[Sr(TETA)]\cdot 5H_2O$, hydrogen atoms were placed on water molecules, and their geometry retained by using the DFIX and the HTAB cards. Space group determination, structure solution, refinement, molecular graphics, and geometrical calculation were carried out for all structures with the SHELXTL software package, release 5.1. Crystal data and structure refinement details are presented in Table 4. CCDC-194130 and CCDC-194131 contain the supplementary crystallographic data for this paper. These data can be obtained free of charge via www.ccdc.cam.ac.uk/conts/retrieving.html (or from the Cambridge Crystallographic Data Centre, 12 Union Road, Cambridge CB2 1EZ, UK; fax: (+44) 1223-336-033; or deposit@ccdc.cam.uk).

Acknowledgement

We thank Prof. András Jánossy, Dr Antal Rockenbauer, and Dr Ferenc Simon, Technical University of Budapest, for the high-field EPR measurements. This research was financially supported by the Swiss National Science Foundation and the Office for Education and Science (OFES). A.S. thanks the CNRS for financial support. This work was carried out in the frame of the EC COST Action D18.

[1] F. Botteman, G. Nicolle, L. Vander Elst, S. Laurent, A. E. Merbach, R. N. Muller *Eur. J. Inorg. Chem.* **2002**, 2686.
[2] V. Jacques, J. F. Desreux in *Topics in Current Chemistry*, *Vol. 221* (Ed.: W. Krause), Springer, Berlin, **2002**.
[3] É. Tóth, L. Helm, A. E. Merbach, *Comprehensive Coordination Chem. II.*, *Vol. 9.* Chap. 9, in press.
[4] S. Aime, M. Botta, E. Gianolio, E. Terreno, *Angew. Chem.* **2000**, *112*, 763; *Angew. Chem. Int. Ed.* **2000**, *39*, 747.
[5] É. Tóth, L. Burai, A. E. Merbach, *Coord. Chem. Rev.* **2001**, *216–217*, 363.
[6] É. Tóth, L. Helm, A. E. Merbach in *Topics in Current Chemistry*, *Vol. 221* (Ed.: W. Krause), Springer, Berlin, 2002.
[7] P. Caravan, É. Tóth, A. Rockenbauer, A. E. Merbach, *J. Am. Chem. Soc.* **1999**, *121*, 10403.
[8] S. Seibig, É. Tóth, A. E. Merbach, *J. Am. Chem. Soc.* **2000**, *122*, 5822.
[9] L. Burai, É. Tóth, S. Seibig, R. Scopelliti, A. E. Merbach, *Chem. Eur. J.* **2000**, *6*, 3761.
[10] L. Burai, R. Scopelliti, É. Tóth, *Chem. Commun.* **2002**, 2366.
[11] R. D. Shannon, *Acta Crystallogr. Sect. A* **1976**, *32*, 751.
[12] A. Varnek, G. Wipff, A. Bilyk, J. M. Harrowfield, *J. Chem. Soc. Dalton Trans.* **1999**, 4155.
[13] P. Starynowicz *Polyhedron*, **1995**, *14*, 3573.
[14] G. Moreau, L. Burai, L. Helm, J. Purans, A. E. Merbach, *J. Phys. Chem. A*, in press.
[15] a) J. P. Dubost, J. M. Leger, M. H. Langlois, D. Meyer, M. C. R. Schaefer, *l'Academie Sci. Ser. II Univers.* **1991**, *312*, 349; b) C. A. Chang, L. C. Francesconi, M. F. Malley, K. Kumar, J. Z. Gougoutas, M. F. Tweedle, D. W. Lee, L. J. Wilson, *Inorg. Chem.* **1993**, *32*, 3501.
[16] J.-G. Kang, M.-K. Na, S.-K. Yoon, Y. Sohn, Y.-D. Kim, I.-H. Suh, *Inorg. Chim. Acta* **2000**, *310*, 56.
[17] R. Ruloff, É. Tóth, R. Scopelliti, R. Tripier, H. Handel, A. E. Merbach, *Chem. Commun.* **2002**, 263.
[18] a) M. R. Spirlet, J. Rebizant, J. F. Desreux, M. F. Loncin, *Inorg. Chem.* **1984**, *23*, 359; b) F. Benetollo, G. Bombieri, S. Aime, M. Botta, *Acta Crystallogr. Sect. C* **1999**, *55*, 353.
[19] J.-G. Kang, M.-K. Na, S.-K. Yoon, Y. Sohn, Y.-D. Kim, I.-H. Suh, *Inorg. Chim. Acta* **2000**, *310*, 56.
[20] D. Eckardt, L. Z. Holleck, *Z. Elektrochem.* **1955**, *59*, 202.
[21] E. L. Yee, O. A. Gansow, M. J. Weaver, *J. Am. Chem. Soc.* **1980**, *102*, 2278.
[22] a) E. T. Clarke, A. E. Martell, *Inorg. Chim. Acta* **1991**, *190*, 27; b) E. T. Clarke, A. E. Martell, *Inorg. Chim. Acta* **1991**, *190*, 37.
[23] L. Burai, I. Fábián, R. Király, E. Szilágyi, E. Brücher *J. Chem. Soc. Dalton Trans.* **1998**, 243.
[24] S. L. Wu, W. D. Horrocks, Jr., *J. Chem. Soc. Dalton Trans.* **1997**, 1497.
[25] G. Anderegg, *Helv. Chim. Acta* **1975**, *58*, 1218.
[26] a) G. Laurenczy, E. Brücher, *Proc. Int. Sympos Rare Earth Spectr.* Wroclaw, **1984**, 127; b) A. E. Martell, R. M. Smith, *Critical Stability Constants*, *Vol. 1*, Plenum Press, New York, **1974**, pp. 281–282.
[27] a) C. A. Chang, M. E. Rowland, *Inorg. Chem.* **1983**, *22*, 3866; b) P. Solymosi, PhD thesis, University of Debrecen, Hungary, **1994**.
[28] É. Tóth, L. Helm, A. E. Merbach "Relaxivity of Gadolinium(III) Complexes: Theory and Mechanism" in *The Chemistry of Contrast Agents in Medical Magnetic Resonance Imaging* (Eds.: É. Tóth, A. E. Merbach), Wiley, Chichester, **2001**. p. 45.
[29] H. D. Powell, O. M. Ni Dhubhghaill, D. Pubanz, Y. S. Lebedev, W. Schlaepfer, A. E. Merbach, *J. Am. Chem. Soc.* **1996**, *118*, 9333.
[30] F. A. Dunand, A. Borel, A. E. Merbach, *J. Am. Chem. Soc.* **2002**, *124*, 710.
[31] a) S. Rast, A. Borel, L. Helm, E. Belorizky, P. H. Fries, A. E. Merbach, *J. Am. Chem. Soc.* **2001**, *123*, 2637; b) S. Rast, P. H. Fries, E. Belorizky, A. Borel, L. Helm, A. E. Merbach, *J. Chem. Phys.* **2001**, *115*, 7554.
[32] a) A. D. McLachlan, *Proc. R. Soc. London A.* **1964**, *280*, 271; b) D. H. Powell, A. E. Merbach, G. González, E. Brücher, K. Micskei, M. F. Ottaviani, K. Köhler, A. von Zelewsky, O. Y. Grinberg, Y. S. Lebedev, *Helv. Chim. Acta* **1993**, *76*, 2129.
[33] A. Borel, L. Helm, A. E. Merbach *Chem. Eur. J.* **2001**, *7*, 600.
[34] G. M. Nicolle, É. Tóth, H. Schmitt-Willich, B. Radüchel, A. E. Merbach, *Chem. Eur. J.* **2002**, *8*, 1040.
[35] H. M. Irving, M. G. Miles, L. D. Petit, *Anal. Chim. Acta* **1967**, *38*, 475.
[36] A. D. Hugi, L. Helm, A. E. Merbach, *Helv. Chim. Acta* **1985**, *68*, 508.
[37] R. V. Vold, J. S. Waugh, M. P. Klein, D. E. Phelps, *J. Chem. Phys.* **1968**, *48*, 3831.
[38] S. Meiboom, D. Gill, *Rev. Sci. Instrum.* **1958**, *29*, 688.
[39] U. Frey, L. Helm, A. E. Merbach, *High Press. Res.* **1990**, *2*, 237.
[40] J. Reuben, *J. Phys. Chem.* **1971**, *75*, 3164.
[41] L. Zékány, I. Nagypál in *Computational Methods for Determination of Formation Constants* (Ed.: D. J. Leggett), Plenum Press, New York, **1985**, p. 291.
[42] Z. Otwinowski, W. Minor in *Methods in Enzymology*, *Vol. 276: Macromolecular Crystallography* (Eds.: C. W. Carter, Jr., R. M. Sweet), Academic Press, **1997**, part A, pp. 307–326.

Received: September 25, 2002 [F4449]

